



Simulation of Surface Plasmon Resonance (SPR) of Silver with Titanium Oxide as a Bi-Layer Biosensor

Farah Jawad Kadhum¹, Shaymaa Hassn Kafi¹, Asrar Abdulmunem Saeed¹, Ali Abid Dawood Al-Zuky¹ and Anwar Hassn Al-Saleh²

¹ Physics Department, College of Science, Mustansiriyah University, Baghdad, Iraq

² Department of Computer Science, College of Science, Mustansiriyah University, Baghdad - Iraq



LINK
<https://doi.org/10.37575/b/sci/210046>

RECEIVED
17/08/2021

ACCEPTED
04/11/2021

PUBLISHED ONLINE
04/11/2021

ASSIGNED TO AN ISSUE
01/12/2021

NO. OF WORDS
4768

NO. OF PAGES
5

YEAR
2021

VOLUME
22

ISSUE
2

ABSTRACT

Surface plasmon resonance (SPR) is a highly sensitive method for monitoring changes in the optical characteristics that are near the sensor surface. It can be stimulated by an evanescent field that comes from the total internal reflection of the backside of the sensor surface in the Otto setup. In this setup, SPR can be used to build a simulation model at different thicknesses of titanium oxide (TiO₂) (dTiO₂ = 50 nm) and silver (Ag) (dAg = 10–80 nm) layers, which are deposited on the semicircular glass prism D-ZLAF50 by using water as a sensing medium. The surface plasmon resonance angle (θ_{SPR}) properties were calculated; SPR was not observed in the ultraviolet region (300 nm) or in the infrared region at 800 nm, but appeared strongly in the visible region at 600 and 700 nm and in the infrared region (900 and 1000 nm). The best sensitivity ($S = 140$) can be observed in the visible region, where the values of SPR dip length (L_d) and full-width half maximum (FWHM) are very good at silver layer thicknesses 40–60 nm; therefore, the proposed sensor can be used in the visible and infrared regions at the wavelengths 600, 700, 900, and 1000 nm.

KEYWORDS

biosensor, liquid sensor, sensitivity, surface plasmons, surface plasmon resonance, theoretical model

CITATION

Kadhum, F.J., Kafi, S.H., Al-Zuky, A.A., Saeed, A.A. and Al-Saleh, A.H. (2021). Simulation of surface plasmon resonance (SPR) of silver with titanium oxide as a bi-layer biosensor. *The Scientific Journal of King Faisal University: Basic and Applied Sciences*, 22(2), 76–80. DOI: 10.37575/b/sci/210046

1. Introduction

Surface plasmon resonance (SPR) is considered an optical phenomenon that is caused by free electron oscillation at the interface between a metallic surface and an insulating layer, where the incident electromagnetic wave's wavelengths coincide with the wavelengths of the surface electrons under p-polarization light (Reather, 1980). When the incident light has a transverse magnetic (TM) polarization (p-polarization) at a given angle on the film metal, the momentum of the incident light equals that of the plasmon, and then resonance occurs; this is known as surface plasmon resonance. Here, the SPR angle is considered the precise angle at which the resonance occurs and the reflected light is damped (Liedberg *et al.*, 1983). Due to their appealing qualities of estimating and exacting the sensing and providing a fast response, real-time detection, and effective label-free lighting control capabilities, SPR sensors have been extensively explored (Nguyen *et al.*, 2015).

Surface plasmon resonance has typically been used to test bio-sensitivity on noble metallic surfaces such as gold and silver. These minerals (or metals) show a few benefits over other types of minerals, as SPR bands are visible and near-infrared frequencies, their surface chemistry is well-defined and easy to manipulate, and films can be made by using several deposition processes (Homola *et al.*, 1999). The most well-known application of SPR is in bio-sensitivity, where biomolecule attachment causes a minor change in the refractive index of the insulated medium near the interface that can be detected by a change in the reflection of the metal surface (Hoa *et al.*, 2007). The resonance angle changes according to the concentration of the target analysis when biomolecules cling to a metal surface (Liedberg *et al.*, 1983). SPR biosensors have been widely used in various analytical research domains due to their advantages, such as their sensitivity, quantitative response, and quick and label-free detection (Shankaran *et al.*, 2007). SPRs dissipate their electromagnetic waves through the metallic layer interaction. Electromagnetic wave loss can be due to the free electron scattering in the plasmonic layer and

optical absorption throughout the electronic inter-band transitions. The sensitivity of SPR measurement varies significantly according to the type of the dielectric (liquid or gas) and the type of configuration (prism, optical fibre, and diffraction grating) (Yang *et al.*, 2018).

Several researchers have studied the SPR sensor system and worked on designing SPR systems that are used as sensors to detect any change in the optical properties of the media under the study.

One of the most important of these studies is Fontana's (2006) Mathcad software that was used to determine the optimum thickness of the deposited layers (Au, Ag, Al, and Cu films) on BK7 glass as the coupling prism material for the maximum SPR sensitivity based on the incident light's wavelength. Another important study by Wu *et al.* (2010) confirmed that the SPR biosensor based on the graphene deposition on gold was more sensitive than the classic SPR thin gold biosensor. The greater absorption of biomolecules onto graphene accounts for its higher sensitivity. In addition, Deng *et al.* (2010) simulated and designed a prism-based SPR sensor by using an Otto configuration, in which a thin layer of gold and another layer (dielectric SiO₂) were deposited on a prism with the use of a 650 nm laser to obtain plasmonic resonance of the layered system. A photodetector monitors the reflected beam as a function of the angle of incidence. The benefits of better SPR detection over traditional detection include a sharper resonance peak and narrower half-width, in addition to better sensitivity, contrast, and detection efficiency. In contrast, Maharana *et al.* (2013) improved the electric field at the sensing layer interface by using graphene as a dielectric overlayer on SPR-active metal Ag.

In comparing what is known as Au and Ag arrangement, we find that their sensor performs better. Rouf and Haque (2018) designed a bimetallic SPR sensor from a pair of silver-gold, in addition to the use of an air gap layer and a thin coating of an indium phosphide. Moreover, they studied different reflectivity curves and performance parameters, and their biosensor was able to detect 1/1000 of the RIU variation medium for the sensing. Lin and Chen (2019) developed an Au-Ag-TiO₂ graphene-based SPR biosensor, demonstrating the

existence of biosensors with a higher sensitivity; meanwhile, the resolution was higher than traditional biosensors. Here, the result shows the effects of the target reflectivity at the resonance angle and prism on the design of an Au-Ag-TiO₂ graphene-based SPR biosensor, in which the biosensor with the BK7 prism has the least refractive index (RI) among the three prisms, and it also has the least FWHM when obtaining $S = 100^\circ/\text{RIU}$. Therefore, it is thought that the proposed genetic algorithm-based design method can be used to improve the performance of an SPR biosensor with any multi-layer structure (Haque *et al.*, 2019). A high-sensitivity SPR sensor on a two-core photonic crystal fibre can detect a low RI. Moreover, a numerical analysis of a two-core, and very sensitive plasmonic refractive index sensor was proposed for low refractive index detection. Akafzade *et al.* (2021) demonstrated a new SPR sensor made from a multi-layer Ag/Si₃N₄/Au nanostructure, which performed admirably at measuring the relative glucose concentrations in glucose/water mixtures. According to computer simulations, the electric field on the surface of this multi-layer sensor is up to 50% greater than on a gold film sensor.

The system that consists of a semicircular D-ZLAF50 glass prism is deposited on two layers, where the first is titanium oxide (TiO₂) with a thickness of 50 nm, and the second is silver (Ag), a thin film with variable thickness from 10 nm to 80 nm. The sensing medium is water, and the complex refractive indices of the materials approved in the study were obtained from the database available on the website refractiveindex.info (Polyanskiy, 2008–2020).

The current work aims to find plasmonic resonance in a wide range of wavelengths and to determine its location in the proposed sensor model's spectral bands by creating a simulation program. The reflectivity of the electromagnetic waves in the range 300 nm to 1000 nm was calculated by adopting Fresnel equations and using a proposed plasmonic resonance transfer matrix.

2. Material and Methods

Surface plasmon resonance occurs when a momentum transfer happens between the evanescent wave that passes through a thin metal layer and a surface plasmon excitation with the same momentum. These waves will be generated if the incident light comes from the side of the plasmonic material, such as glass, and has a higher refractive index, such that at a specific angle, the optical absorption of incidence light will increase. When this angle equals the SPR angle of the specific material and wavelength, the plasmonic dip height will reach the maximum (i.e. the minimum reflectivity). The reflectivity of the plasmonic film can be normal at all angles except for short-range SPR angles (θ_{SPR}), where the absorption reaches the maximum point. The maximum absorption will occur when the incident light's wave vector coincides with the surface plasmons' wave vector (Bhowmik *et al.*, 2016).

A multi-layer structure's reflectance and transmittance can be measured by using the transfer matrix method. In contrast, the traditional transfer matrix implies coherent light propagation, but results in narrow oscillations in a system's observed reflectance and transmittance spectra. These oscillations are not visible in practice due to interference-destroying effects. As a result, interference-destroying effects should be included to provide a practical explanation of the optical properties of multi-layer systems.

All past attempts to alter the transfer matrix to accommodate an incoherent intervention and partial coherence failed. The square of an amplitude of the electric field or Fresnel coefficients are used in the proposed methods to analyse the incoherent event. In partial coherence, the macroscopic surface or the interface roughness

simulation is achieved by multiplying the Fresnel coefficients with the correction factors (Bhowmik *et al.*, 2016).

Fresnel's Equations are used to calculate the reflectivity of the material's multiple layers that are deposited on a given surface, where the electric and magnetic field amplitudes on the first boundary (E_a & H_a) and the N-layer model are connected to those on the last boundary (E_N & H_N) through the total characteristic matrix (Ouyang *et al.*, 2016):

$$\begin{bmatrix} E_a \\ H_a \end{bmatrix} = \left[\prod_{i=1}^N M_i \right] \begin{bmatrix} E_N \\ H_N \end{bmatrix} = \begin{bmatrix} m_{11} & m_{12} \\ m_{21} & m_{22} \end{bmatrix} \begin{bmatrix} E_N \\ H_N \end{bmatrix} \quad (1)$$

M_i : is an actual transfer matrix of the i -th layer ($i = 1$ to N), arranged in sequential order between a prism and a sensing layer, and it is calculated through the following (Shalabney and Abdulhalim, 2010):

$$M_i = \begin{bmatrix} \cos\delta_i & i\sin\delta_i \\ i\gamma_i\sin\delta_i & \cos\delta_i \end{bmatrix} \quad (2)$$

In this case, the optical phase addition caused by a single field passage over the layer, δ_i , is given by the following (Bhowmik *et al.*, 2016):

$$\delta_i = \left(\frac{2\pi}{\lambda} \right) n_i d_i \cos\theta_i \quad (3)$$

Where λ : is the wavelength of incident light in a vacuum, n_i is a refractive index, d_i is a thickness, and θ_i is the incidence angle of the i -th layer. For p-polarization, the parameter for each layer γ_i is the following (Shalabney and Abdulhalim, 2010):

$$\gamma_i = \frac{n_i \sqrt{\epsilon_0 \mu_0}}{\cos\theta_i} \quad (4)$$

Where ϵ_0 : the vacuum permittivity, and μ_0 : the permeability.

When we test several layers in thin films, it appears that the CTM method's strength is better estimated. The electric and magnetic fields within the i -th layer with both interfaces were related to an interference matrix M_i at that layer in Eq. (1). The total interference matrix of the entire multi-layer structure was obtained by using M because the electrical and magnetic fields' transverse components appear at any interface that is free of a net charge and current. The reflection and transmission indices (r and t) through the films may be calculated as follows (Shalabney and Abdulhalim, 2010):

$$r = \frac{\gamma_N m_{11} + \gamma_0 \gamma_N m_{12} - m_{21} - \gamma_0 m_{22}}{\gamma_N m_{11} + \gamma_0 \gamma_N m_{12} + m_{21} + \gamma_0 m_{22}} \quad (5)$$

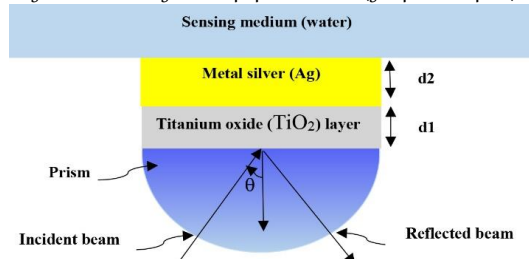
$$t = \frac{2\gamma_0 \left(\frac{n_N}{n_0} \right)}{\gamma_N m_{11} + \gamma_0 \gamma_N m_{12} + m_{21} + \gamma_0 m_{22}} \quad (6)$$

From Eq. (5), the multi-layer stack's reflectance $R = |r|^2$ can be determined to get an incident light energy pattern redistribution. As a result, reflected field power as a function of incident angle was converted into SPR waves. Eq. (6) may be also used to measure the transmission across a multi-layer stack $T = |t|^2$.

Figure 1 shows a schematic design of the proposed SPR sensor. All metals have complex dielectric constants, and the metals with a larger negative real fraction and smaller positive imaginary fraction have good plasmonic effects. When electronic excitation occurs, the light will be absorbed. Silver is chemically stable and interacts very poorly with the atmosphere and other chemicals. It is optically transparent in the range of UV to IR 250–900 nm, and it has a relatively large refractive index, as well as thermal stability, hardness, chemical inertness, a low cost, and good chemical stability (Santos *et al.*, 2013). A good and stable plasmon sense system can be constructed by

depositing a thin layer of the silver on a prism (Gupta and Sharma, 2005). The response of this sensing system to the gases and liquids can be increased by depositing an additional layer of TiO_2 because the dielectric layer of titanium oxide provides many exceptional properties. At the interface between the superoxide layer and the sensor medium, the TiO_2 also increases the local electron field strength. Any change in the refractive index of the sensing medium or an increase in the electronic field strength causes an increase in the shift of the SPR wavelength, which therefore results in an improved sensitivity (Díaz-Herrera *et al.*, 2010).

Figure 1: Schematic diagram of the proposed SPR sensor (glass prism half-sphere).



In the simulation steps, an electromagnetic wave with wavelengths ranging from 300 nm to 1000 nm was adopted to find the spectrum regions where the SPR phenomenon occurs. In this study, an Otto configuration with a D-ZLAF50 glass half sphere prism was used. A layer of TiO_2 with a constant thickness of 50 nm was deposited on the prism, and then another layer of Ag with a different thickness (10–80 nm) was deposited, with water used as a medium for biological or chemical sensitivity. The SPR dip must be deep enough, sharp, and in high contrast for the sensor in order to be effective and good. A very wide SPR dip indicates the possibility of a wider range of an incident SPR angle, and thus it makes the sensitivity of the sensor worse. In summary, these parameters were changed during the simulation:

- Electromagnetic waves: wavelengths ranging from 300 nm to 1000 nm with step changes 100 nm from ultraviolet wavelength to near-infrared wavelength.
- The amount of change in the refractive index of the external sensing medium in contact with the sensor: ($\Delta n = 0, 0.02, 0.05, \text{ and } 0.1$).
- Dielectric (TiO_2) layer thickness constant $d_{\text{TiO}_2} = 50$ nm.
- Silver layer thickness: (10–80) nm with step changes 10 nm.

An important note is that as the incident wavelengths change, the refractive indices of the system materials ((prism D-ZLAF50) glass, dielectric (TiO_2), silver, and water) will change. The simulation program was performed by developing Yamamoto's algorithms in 'Surface Plasmon Resonance (SPR) Theory' (Yamamoto, 2002).

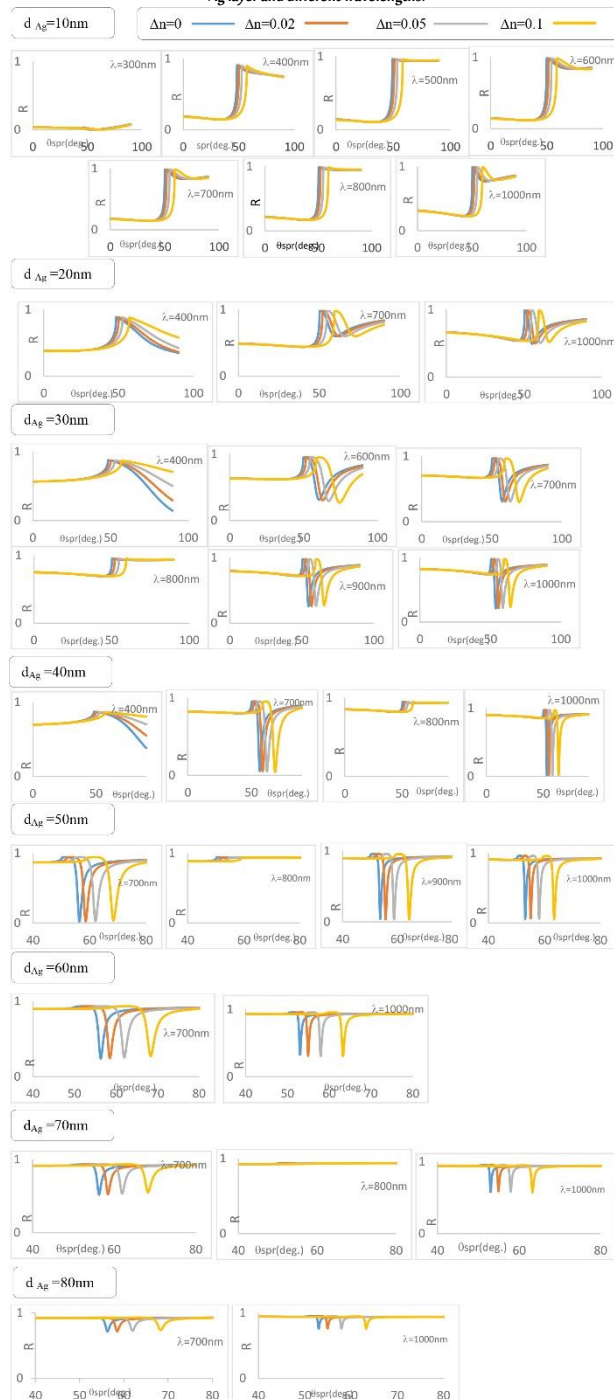
3. Results and Discussion

The optimum film thickness of the metal-based SPR sensor has the SPR reflectivity curve produced by a sensor structure that shows the maximum possible loss in the reflectivity. It also produces the narrowest possible FWHM of the SPR dip, with the length of the SPR dip close to one. Figure 2 shows the reflectivity curves for the TiO_2 50 nm thickness layer, and Ag of thickness varying from 10 nm to 80 nm with steps 10 nm. It is identified by the angle of the surface plasmon resonance (θ_{SPR}). The angle of the incidence at which the minimum reflection occurs corresponds to the maximum energy loss due to the excitation of the surface plasmon. The characteristics of the reflectivity curves and the occurrence of SPRs can be summarized as follows:

- By using a silver thickness of 10 nm and 20 nm, there are no instances of SPR that can be used in the sensing process. For 30 nm thickness, the SPR states began to appear at the wavelengths of 600 nm, the state of SPR improved at the wavelength of 700 nm, the state of SPR completely disappeared at the wavelength of 800 nm, but it appeared strongly at the wavelengths 900 nm and 1000 nm.

- SPRs become very strong by using silver with a thickness between 40 nm and 50 nm, they weaken slightly at 60 nm thickness, and they are even weaker at 70–80 nm silver thickness for all used wavelengths.
- The SPR angle shifted slightly towards the higher values with an increase in the refractive index of the sensing medium Δn ; this agrees with Deng and Liu (2010).

Figure 2: Shows the relation between the reflectance in the incident angle of the different thickness Ag layer and different wavelengths.



The computed SPR dip properties – FWHM and the height (L_d) and the best SPR sensor that gives a sharper FWHM and longer L_d and that approaches one – also compute the sensor sensitivity by using the following (Seo *et al.*, 2017):

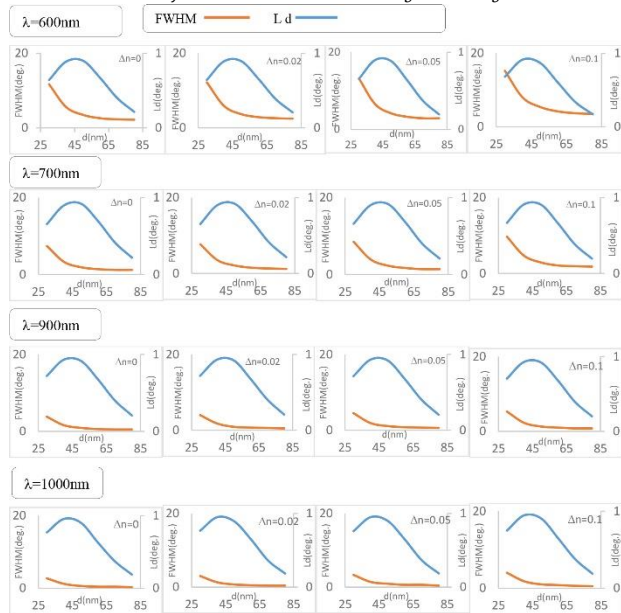
$$S = \frac{\Delta \theta_{\text{SPR}}}{\Delta n_{\text{dIo}}} \quad (8)$$

Figure 3 illustrates the computed FWHM and the length (L_d) of the

SPR dip with the change in the outer medium refractive index.

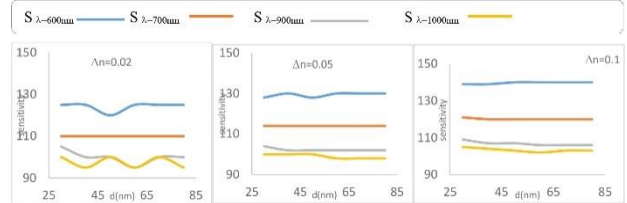
It is noted that the FWHM for the SPR dip is gradually decreasing in all cases with an increased silver thickness, but the best cases were those using the wavelengths 1000 nm and 900 nm. It was also observed that the SPR dip length (L_d) increased till it reached its peak at the silver thickness between 40 nm and 60 nm, and then it gradually decreased when the silver thickness increased. This information helped determine the best silver thickness for use in the sensor. This happens when the FWHM is rather small and the SPR dip length (L_d) is large, and it helps achieve the sensing purpose of the sensor. This was achieved within a silver thickness range of 40 nm to 60 nm. The value ranges in this silver thickness (d_{Ag}) were as follows: the L_d were $\cong 0.8$ – 0.9 for the wavelengths 600, 700, 900, and 1000 nm, and the best values for the L_d were for the SPR dip length at the wavelengths of 900 and 1000 nm and $\Delta n=0.1$. As for the FWHM values when using $\Delta n=0.1$ with the 600 nm wavelength within 15.2–3.5 degrees in a changing of d_{Ag} , the FWHM values improved, and the SPR dip became narrower when using the 700 nm wavelength, with its value becoming 9.7–1.8 degrees with different d_{Ag} . Then, the FWHM began to decrease further, which means that the SPR dip became narrower when using the wavelength 1000 nm, and its FWHM value became 4–0.5 degrees with different d_{Ag} .

Figure 3: Shows the Full-Width Half Maximum (FWHM) and length dip L_d with the change refractive index of layer thin films for different thickness Ag and wavelengths.



The relationship between sensitivity related to the changing thickness of the Ag layer and the refractive indices of sensing medium $\Delta n = (0.02, 0.05, \text{ and } 0.1)$ is shown in Figure 4, where the relationship between sensitivity and change in the silver thicknesses was stable for all thickness ranges. However, the sensitivity was highest at 600 nm, followed by 700 nm, 900 nm, and 1000 nm. It can also be noted that the sensitivity increases with the increase of the change in the refractive index of the sensing medium Δn . The best sensitivity values (S) were when using the wavelength $\lambda = 600$ nm, where its values ranged between $S = 102$ and 140 for thicknesses from $d_{Ag} = (30$ – $80)$ nm and $\Delta n = 0.1$, which agrees with research by Rouf and Haque (2018).

Figure 4: Illustrates the sensitivity related to thicknesses of Ag layers at a different wavelength with the refractive index Δn .



The proposed system can be adopted as an effective biological sensor within the visible-infrared spectrum region at a wavelength of 600, 700, 900, and 1000 nm.

4. Conclusions

Form the results of this study, the following points are concluded:

- When applying the simulation algorithm to the proposed sensor in this study, it is observed that the SPR phenomenon cannot appear in the ultraviolet region, but it appears weakly in the visible region, starting at a wavelength of 600 nm, and then it is improved further at a wavelength of 700 nm. While in the infrared region, SPR disappears completely at a wavelength of 800 nm and appears strongly at the wavelengths 900 nm and 1000 nm.
- In the visible region of the spectrum, the best working stability of the sensor is obtained at a wavelength of 600 nm. Where the sensitivity is obtained with values of $S = 102$ – 140 , the SPR dip length is within the limits of $L_d \cong (0.8$ – $0.9)$ and $\text{FWHM} = 15.2$ – 3.5 degrees, for thickness, and $d = 30$ – 80 nm, for sensing the change of the refractive index of the Aqueous medium ranges between $\Delta n = 0.01$ – 0.1 .
- In the infrared region, the values of SPR dip length (L_d) and full-width half maximum (FWHM) are very good at the silver layer thicknesses 40–60 nm. The best values for the L_d were $\cong (0.8$ – $0.9)$ for the SPR dip length at the wavelengths 900 and 1000 nm and $\Delta n = 0.1$. After that, the FWHM begins to decrease further, which means that the SPR dip becomes narrower when using the wavelength 1000 nm, and its FWHM value becomes 4–0.5 degrees with different d_{Ag} .

The proposed system can be used as an effective biosensor within the visible and infrared spectral regions of wavelengths 600, 700, 900 and 1000 nm at a silver layer thickness of 40 to 60 nm.

Acknowledgements

The authors would like to thank Department of Physics/ College of Science/ Mustansiriya University (www.uomustansiriya.edu.iq) Baghdad-Iraq for its support in the present work.

Biographies

Farah Jawad Kadhum

Department of Physics, College of Science, Al-Mustansiriya University, Baghdad, Iraq, farahjawadlnuaimi@uomustansiriya.edu.iq, 009647704535571

Mrs Kadhum is an Iraqi assistant Professor. She has a master's degree in physics from the Department of Applied Sciences, Al-Technology University, Iraq. Her field of interest is material physics and she has published more than 30 articles in global, regional, and local scientific journals. Some papers are in Scopus and Clarivate indices in the fields of material physics, polymer and laser dyes, spectroscopy, and molecular physics. She has participated in several local and regional seminars, workshops, and conferences. ORCID: 0000-0002-7188-8823

Shaymaa Hassan Kafi

Department of Physics, College of Science, Al-Mustansiriya University, Baghdad, Iraq, shaymaa.h.kafi@uomustansiriya.edu.iq, 0096477995787

Mrs Kafi is an Iraqi assistant lecturer at the Department of Physics, College of Science, Al-Mustansiriya University. She obtained her master's degree in physics from the College of Science, Al-

Mustansiriyah University, Iraq. Her specialization is optics. She has published more than 10 articles in global, regional, and local scientific magazines; some are in Scopus and Clarivate indices in the field of optics physics. She has participated in several local and regional seminars, workshops, and conferences. She has received many certificates of appreciation for her active participation in training workshops. ORCID: 0000-0003-0737-6580

Asrar Abdulmunem Saeed

Department of Physics, College of Science, Al-Mustansiriyah University, Baghdad, Iraq, dr.asrar@uomustansiriyah.edu.iq, 009647707782082

Dr Saeed is an Iraqi assistant professor at the Department of Physics, College of Science, Al-Mustansiriyah University. She has a PhD degree in physics from the Department of Physics, College of Science, Baghdad University. She specializes in material physics. She supervises several postgraduate master's and doctoral students. She has published more than 30 articles in global, regional, and local scientific magazines; some are in Scopus and Clarivate indices in the fields of material physics, polymer and laser dyes, spectroscopy, and molecular physics. ORCID: 0000-0003-4677-7598

Ali Abid Dawood Al-Zuky

Department of Physics, College of Science, Al-Mustansiriyah University, Baghdad, Iraq, prof.aliazuky@uomustansiriyah.edu.iq, 009647706040619

Dr Al-Zuky is an Iraqi professor at the Department of Physics, College of Science, Al-Mustansiriyah University. He has a PhD degree in physics from the Department of Physics, College of Science, University of Baghdad, Iraq. He specializes in digital image processing and artificial intelligence. He has supervised more than 50 postgraduate students in the fields of physics, computers, computer engineering, and medical physics. He has published more than 150 scientific papers in scientific magazines and conferences. He has received many certificates of appreciation for his active participation in training workshops. ORCID: 0000-0002-3087-3908

Anwar Hassan Al-Saleh

Department of Computer Science, College of Science, Al-Mustansiriyah University, Baghdad, Iraq, anwar.h.m@uomustansiriyah.edu.iq, 009647707782082

Mrs Al-Saleh is an Iraqi assistant Professor at the Department of Computer Science, College of Science, Al-Mustansiriyah University. She obtained a master's degree in computer science from the College of Science, Al-Mustansiriyah University, Iraq. She specializes in image processing and has published more than 20 articles in global, regional, and local scientific magazines; some are in Scopus and Clarivate indices in the field of image processing. She has participated in several local and regional seminars, workshops, and conferences. ORCID: 0000-0001-9833-7119

References

- Akafzade, H., Hozhabri, N. and Sharma, S.C. (2021). Highly sensitive plasmonic sensor fabricated with multi-layer Ag/Si₃N₄/Au nanostructure for the detection of glucose in glucose/water solutions. *Sensors and Actuators A: Physical*, **317**(n/a), 112430.
- Bhowmik, B., Manjuladevi, V., Gupta, R. and Bhattacharyya, P. (2016). Highly selective low-temperature acetone sensor based on hierarchical 3-D TiO₂ nanoflowers. *IEEE Sensors Journal*, **16**(10), 3488–95.
- Deng, Y. and Liu, G. (2010). Surface plasmons resonance detection based on the attenuated total reflection geometry. *Procedia Engineering*, *Elsevier*, **7**(n/a), 432–5.
- Díaz-Herrera, N., González-Cano, A., Viegas, D.C. and Santos, J.L. (2010). Refractive index sensing of aqueous media based on plasmonic resonance in tapered optical fibres operating in the 1.5 μ m region. *Sensors and Actuators B: Chemical*, **146**(1), 195–8.
- Fontana, E. (2006). Thickness optimization of metal films for the development of surface-plasmon-based sensors for nonabsorbing media. *Applied Optics*. *Optical Society of America*, **45**(29), 7632–42.
- Gupta, B.D. and Sharma, A.K. (2005). Sensitivity evaluation of a multi-layered surface plasmon resonance-based fiber optic sensor: A theoretical study', *Sensors and Actuators B: Chemical*, **107**(1), 40–6.
- Haque, E., Mahmuda, S., Hossain, M.A., Hai, N.H., Namihira, Y. and Ahmed, F. (2019). Highly sensitive dual-core PCF based plasmonic refractive index sensor for low refractive index detection. *IEEE Photonics Journal*, **11**(5), 1–9.
- Hoa, X.D., Kirk, A.G. and Tabrizian, M. (2007). Towards integrated and sensitive surface plasmon resonance biosensors: A review of recent progress. *Biosensors and bioelectronics*. *Elsevier*, **23**(2), 151–60.
- Homola, J., Yee, S.S. and Gauglitz, G. (1999). Surface plasmon resonance sensors. *Sensors and Actuators B: Chemical*, **54**(1–2), 3–15.
- Liedberg, B., Nylander, C. and Lunström, I. (1983) Surface plasmon resonance for gas detection and biosensing. *Sensors and Actuators*, **4**(n/a), 299–304.
- Lin, C. and Chen, S. (2019). Design of high-performance Au-Ag-dielectric-graphene based surface plasmon resonance biosensors using genetic algorithm. *Journal of Applied Physics*, **125**(11), 113101.
- Maharana, P.K. and Jha, R. (2013/12/17-18). Enhancing performance of SPR sensor through electric field intensity enhancement using graphene. In: *Workshop on Recent Advances in Photonics (WRAP)*, IEEE, pp. 1–2, New Delhi, India.
- Nguyen, H.H., Park, J., Kang, S. and Kim, M. (2015). Surface plasmon resonance: A versatile technique for biosensor applications. *Sensors*, *Multidisciplinary Digital Publishing Institute*, **15**(5), 10481–510.
- Ouyang, Q., Zeng, S., Jiang, L., Hong, L., Xu, G., Xuan-Quyem, D., Qian, J., He, S., Qu, J., Coquet, P. and Ken-Tye Y. (2016). Sensitivity enhancement of transition metal dichalcogenides/silicon nanostructure-based surface plasmon resonance biosensor. *Nature Publishing Group*, **6**(1), 1–13.
- Polyanskiy, M. (2008-2020). *Refractive Index*. Available at: <https://refractiveindex.info> (accessed on 10/08/2021).
- Reather H., (1980). *Excitation of Plasmons and Interband Transitions by Electrons*. Springer: Berlin, Germany.
- Rouf, H.K. and Haque, T. (2018). Performance Enhancement of Ag-Au Bimetallic Surface Plasmon Resonance Biosensor using InP. *Progress in Electromagnetics Research*, **76**(n/a), 31–42.
- Santos, D.F., Guerreiro, A. and Baptista, J.M. (2013). Numerical investigation of a refractive index SPR D-type optical fiber sensor using COMSOL multiphysics. *Photonic Sensors*. *Springer*, **3**(1), 61–6.
- Seo, M., Lee, J. and Lee, M. (2017). Grating-coupled surface plasmon resonance on bulk stainless steel. *Optics Express*, *Optical Society of America*, **25**(22), 26939–49.
- Shalabney, A. and Abdulhalim, I. (2010). Electromagnetic fields distribution in multi-layer thin film structures and the origin of sensitivity enhancement in surface plasmon resonance sensors. *Sensors and Actuators A: Physical*, **159**(1), 24–32.
- Shankaran, D.R., Gobi, K.V. and Miura, N. (2007). Recent advancements in surface plasmon resonance immunosensors for detection of small molecules of biomedical, food and environmental interest. *Sensors and Actuators B: Chemical*, **121**(1), 158–77.
- Wu, L., Chu, H.S., Koh, W.S. and Li, E.P. (2010). Highly sensitive graphene biosensors based on surface plasmon resonance. *Optics express* *Optical Society of America*, **18**(14), 14395–400.
- Yamamoto's, M. (2002). Surface Plasmon Resonance (SPR) Theory. *Review of Polarography*, **48**(3), 209–37
- Yang, L., Wang, J., Li-zhi, Y. and Zheng-Da, H. (2018). Characteristics of multiple Fano resonances in waveguide-coupled surface plasmon resonance sensors based on waveguide theory. *Scientific Reports*, **8**(1), 1–10.